

Orbital-selective Mott phase of Cu-substituted iron-based superconductors

Yang Liu, Yang-Yang Zhao, and Yun Song

Department of Physics, Beijing Normal University, Beijing 100875, China

E-mail: yunsong@bnu.edu.cn

Abstract. We study the phase transition in Cu-substituted iron-based superconductors with a new developed real-space Green's function method. We find that Cu substitution has strong effect on the orbital-selective Mott transition introduced by the Hund's rule coupling. The redistribution of the orbital occupancy which is caused by the increase of the Hund's rule coupling, gives rise to the Mott-Hubbard metal-insulator transition in the half-filled d_{xy} orbital. We also find that more and more electronic states appear inside that Mott gap of the d_{xy} orbital with the increase of Cu substitution, and the in-gap states around the Fermi level are strongly localized at some specific lattice sites. Further, a distinctive phase diagram, obtained for the Cu-substituted Fe-based superconductors, displays an orbital-selective insulating phase, as a result of the cooperative effect of the Hund's rule coupling and the impurity-induced disorder.

PACS numbers: 74.20-z, 74.70.Xa, 74.62.Dh, 71.30.+h

1. INTRODUCTION

The multiorbital nature of iron pnictides and chalcogenides is essential for understanding the mechanism of the high-temperature superconductivity of iron-based superconductors [1, 2]. The multiple Fe $3d$ orbitals, which couple strongly with each other by the Hund's rule exchange interaction, contribute most to the low-energy excitations [3, 4, 5]. Some theoretical studies showed that the Hund's rule coupling plays a key role in tuning the degree of electronic correlation in multiorbital systems [6, 7, 8, 9]. Using a slave-spin method, it was predicted that an orbital-selective Mott phase (OSMP) will emerge in $K_{1-x}Fe_{2-y}Se_2$ when the Hund's rule coupling exceeds a certain threshold value [10]. Experimentally, strong orbital-dependence of the correlation was found in iron chalcogenides [11], and the signs of the appearance of OSMP were also observed in $A_xFe_{2-y}Se_2$ ($A=K, Rb$) at high temperature [12, 13, 14].

It has been demonstrated by the dynamical mean-field theory (DMFT) [15] that, in a multiorbital system, the OSMP is usually derived from three possible reasons: (1) the bandwidths of the two orbitals are significantly different [16]; (2) the influence of the crystal-field splitting is considerable [17]; and (3) the orbital degeneracy is reduced owing to the distinct features of the orbitals or by some other reasons [18, 19]. However, it is still unclear whether the OSMP is sensitive to the effect of disorder introduced by impurities. In iron-based superconductors, many experiments were implemented by substituting Fe with other transition metals [20, 21, 22, 23, 24, 25, 26, 27, 28, 29, 30], which not only affects the carrier density of the system, but also introduces the effect of disorder. Among various transition-metal substitutions, Cu doping is highly disruptive to the electron structures of the FeAs sheets. In this paper, we will focus on the effect of Cu substitution in Fe-based superconductors, especially the cooperative effect of the Hund's rule coupling and the impurity-induced disorder on the OSMP.

It is still a theoretical challenge to study the multiorbital correlation and the effect of disorder on equal footing [31]. To precisely study the real-space fluctuations introduced by Cu substitution, we develop a real-space Green's function method by extending the Hubbard-I approximation [32] to the multiorbital Hubbard model. Our decoupling approximation has been proved to be adequate for the study of Cu-substituted iron-based superconductors [33]. In accordance with the prediction of other theoretical studies [7, 8, 10], we find an OSMP tuned by the Hund's rule coupling in the undoped cases, where the d_{xy} orbital is a Mott insulator while the d_{xz}/d_{yz} orbitals remain itinerant. In the presence of the Cu substitution, the competition between the Mott-Hubbard and Anderson metal-insulator transitions (MIT) is revealed by the study of the interplay between the Hund's rule coupling and the impurity-induced disorder in Cu-substituted Fe-based superconductors. We find that the Cu substitutions can introduce some states inside the Mott gap of the d_{xy} orbital around the Fermi level, which can be suppressed by the increasing Hund's rule coupling. As a result, the increase of the critical value for the Mott-Hubbard MIT transition is found in the d_{xy} orbital. Meanwhile, the degenerate d_{xz}/d_{yz} orbitals are Anderson localized, indicating the existence of an orbital-selective

insulating phase in Fe-based superconductors with the presence of impurities. We also construct a complete phase diagram for Cu-substituted iron-based superconductors, depended on both the Hund's rule coupling and the concentration of Cu impurities.

The paper is organized as follows. In section 2, we introduce an inhomogeneous three-orbital Hubbard model, and develop a real-space Green's function approach to study the cooperative effect of disorder and multiorbital correlation in Cu-substituted Fe-based superconductors. In section 3, we first show the orbital-selective Mott transition (OSMT) introduced by the Hund's rule coupling in undoped compound. Then we study the cooperative effect of the Hund's rule coupling and impurity-induced disorder on the phase transitions in Cu-substituted iron-based superconductors. Further, a phase diagram is obtained by the study of the competition between the Mott-Hubbard and Anderson MITs. The principal findings of this paper are summarized in section 4.

2. Model Hamiltonian and Methodology

An inhomogeneous three-orbital Hubbard model is introduced for the Cu-substituted Fe-based compounds based on the local density functional calculations of $\text{NaFe}_{1-x}\text{Cu}_x\text{As}$ [33], where a certain percentage of Fe sites is replaced by Cu ions randomly. The Hamiltonian is expressed as

$$\begin{aligned}
H = & - \sum_{i \neq j (i, j \in \text{Fe})} \sum_{\alpha\beta\sigma} T_{i\alpha, j\beta} c_{i\alpha\sigma}^\dagger c_{j\beta\sigma} - \sum_{i \neq j (i, j \in \text{Cu})} \sum_{\alpha\sigma} t_{ij} c_{i\alpha\sigma}^\dagger c_{j\alpha\sigma} \\
& - \sum_{i \in \text{Fe}, j \in \text{Cu}} \sum_{\alpha\beta\sigma} t'_{ij} c_{i\alpha\sigma}^\dagger c_{j\beta\sigma} - \mu \sum_{i\alpha\sigma} n_{i\alpha\sigma} + \Delta_{xy} \sum_{i \in \text{Fe}, \sigma} n_{i, xy, \sigma} \\
& + U \sum_{i \in \text{Fe}, \alpha} n_{i\alpha\uparrow} n_{i\alpha\downarrow} + \sum_{i \in \text{Fe}} \sum_{\alpha < \beta, \sigma\sigma'} (U' - J\delta_{\sigma\sigma'}) n_{i\alpha\sigma} n_{i\beta\sigma'} \\
& + u \sum_{i \in \text{Cu}, \alpha} n_{i\alpha\uparrow} n_{i\alpha\downarrow}, \tag{1}
\end{aligned}$$

where $c_{i\alpha\sigma}^\dagger$ ($c_{i\alpha\sigma}$) creates (annihilates) an electron with spin projection σ for orbital α (d_{xz} , d_{yz} , or d_{xy}) of an iron or copper site i . $T_{i\alpha, j\beta}$ is the hopping term within orbitals α and β between nearest-neighbor (NN) or next-nearest-neighbor (NNN) iron sites i and j . t_{ij} represents the intraorbital hopping integral between NN copper atoms, and t'_{ij} denotes the hopping between NN Cu and Fe ions. U and U' are the onsite intraorbital and interorbital Coulomb interactions on iron sites respectively, and $\Delta_{xy} = \mu_{xy} - \mu_{xz}$ is the energy splitting between the d_{xy} and the degenerate d_{xz}/d_{yz} orbitals. Further, J represents the Ising-type Hund's rule couplings for Fe atoms, and u is the intraorbital interaction of Cu ions.

The values of the tight-binding (TB) model parameters were determined by the first principle calculations of the undoped Fe-based compounds [34, 35]. The local density function calculation predicted that the Fermi surfaces of $\text{NaFe}_{1-x}\text{Cu}_x\text{As}$ are mainly composed by three Fe 3d orbitals, i.e. d_{xy} , d_{xz} and d_{yz} orbitals, whereas Cu 3d orbitals distribute from -4 eV to -2 eV, which is far below the Fermi level [33]. Therefore,

Table 1. Every single term of the nearest neighbor and next nearest neighbor hoppings (T_{NN} and T_{NNN}) for the Fe ions of the tight-binding Hamiltonian in Eq. (1). $(-1)^{|i|}$ indicates that the hopping parameters change sign along the site locations, arising from the two-iron unit cell of the original FeAs planes [34].

T_{NN}	$[1, 0]$	$[0, 1]$	$[-1, 0]$	$[0, -1]$
(d_{xy}, d_{xy})	T_1	T_1	T_1	T_1
(d_{xy}, d_{xz})	$(-1)^{ i }T_3$	0	$(-1)^{ i+1 }T_3$	0
(d_{xy}, d_{yz})	0	$(-1)^{ i }T_3$	0	$(-1)^{ i+1 }T_3$
(d_{xz}, d_{xz})	T_6	T_5	T_6	T_5
(d_{yz}, d_{yz})	T_5	T_6	T_5	T_6
(d_{yz}, d_{xz})	0	0	0	0
T_{NNN}	$[1, 1]$	$[-1, 1]$	$[-1, -1]$	$[1, -1]$
(d_{xy}, d_{xy})	T_2	T_2	T_2	T_2
(d_{xy}, d_{xz})	$(-1)^{ i+1 }T_4$	$(-1)^{ i }T_4$	$(-1)^{ i }T_4$	$(-1)^{ i+1 }T_4$
(d_{xy}, d_{yz})	$(-1)^{ i+1 }T_4$	$(-1)^{ i+1 }T_4$	$(-1)^{ i }T_4$	$(-1)^{ i }T_4$
(d_{xz}, d_{xz})	T_7	T_7	T_7	T_7
(d_{yz}, d_{yz})	T_7	T_7	T_7	T_7
(d_{yz}, d_{xz})	$-T_8$	T_8	$-T_8$	T_8

the Fermi surfaces should be very sensitive to the hopping terms within the three Fe $3d$ orbitals. In the undoped case, our TB model for iron sites is exactly the same as the three-orbital TB Hamiltonian introduced by Daghofer *et al.* for the pnictides followed the Slater-Koster procedure [34, 35]. In Table 1, we display the details about the definitions of the intraorbital and interorbital hopping integrals $T_{i\alpha,j\beta}$ for d_{xy} , d_{xz} and d_{yz} orbitals of Fe ions. Further details about the model parameters can also be found in Ref. [33].

Although the correlations in various iron-based compounds are different, it is generally believed that the correlations should be smaller than the bandwidths. The parameters of the intraorbital and interorbital interactions of the three-orbital Hubbard model (Eq. (1)) have been obtained by the best fitting of the Fermi surfaces with the experimental result of LiFeAs [36], that is $U=1.5$ eV and $U'=1.125$ eV [33]. However, some study also suggested that the Hund's rule coupling in iron-based superconductors should be within $U/10$ and $U/5$ [6]. Therefore, it is important to find out what is the influence of different values of J on the properties of Fe-based superconductors. Because

the main purpose of this paper is to explore the cooperative effects of the Hund's rule coupling and the doping-induced disorder, we fix the value of U as 1.5 eV in the following calculations. The values of the TB model parameters and the multiorbital correlations of the three-orbital Hubbard model are shown in Table 2.

Table 2. Values of the model parameters of the inhomogenous three-orbital Hubbard model. The energy unit is electron volts.

T_1	T_2	T_3	T_4	T_5	T_6	T_7	T_8
0.15	0.15	-0.12	0.06	-0.08	0.1825	0.08375	-0.03
t	t'	Δ_{xy}	U	U'	J	u	
0.01	0.01	0.75	1.5	0.9~1.5	0~0.3	3 or 6	

We study the inhomogeneous three-orbital Hubbard model by a newly developed real-space Green's function method [33]. In this approach, we generalize hundreds of disorder configurations for each Cu concentration, and the final physical properties, such as the density of states (DOS) and conductivity, are obtained by the arithmetical average of the results for different samples. For a certain disorder sample of a square lattice with $N = L^2$ sites, we randomly choose N_{imp} ($N_{imp} = N \times x$) sites to put the Cu ions when the concentration of Cu substitution is x . To exactly study the effect of disorder, we construct a complete real-space Green's function \mathbf{G} , which can be expressed as a $3N \times 3N$ matrix with elements defined as

$$G_{ij\sigma}^{\alpha\beta} = \langle \langle c_{i\alpha\sigma} | c_{j\beta\sigma}^\dagger \rangle \rangle. \quad (2)$$

The equation of motion of each element of the Green's function \mathbf{G} can be obtained by [37]

$$\omega \langle \langle A | B \rangle \rangle = \langle [A, B]_+ \rangle + \langle \langle [A, H] | B \rangle \rangle. \quad (3)$$

Applying the Hamiltonian of Eq. (1) to the above equation, we obtain the equation of motion of $G_{ij\sigma}^{\alpha\beta}$ as

$$\begin{aligned} (\omega + \mu_\alpha) \langle \langle c_{i\alpha\sigma} | c_{j\beta\sigma}^\dagger \rangle \rangle &= \delta_{ij} \delta_{\alpha\beta} - \sum_{b \in Fe, m} T_{ib\alpha m} \langle \langle c_{bm\sigma} | c_{j\beta\sigma}^\dagger \rangle \rangle \\ &\quad - \sum_{b \in Cu, \gamma} t'_{ib} \langle \langle c_{b\gamma\sigma} | c_{j\beta\sigma}^\dagger \rangle \rangle + U \langle \langle n_{i\alpha\bar{\sigma}} c_{i\alpha\sigma} | c_{j\beta\sigma}^\dagger \rangle \rangle \\ &\quad + U' \sum_{l \neq \alpha} \langle \langle n_{il\bar{\sigma}} c_{i\alpha\sigma} | c_{j\beta\sigma}^\dagger \rangle \rangle + (U' - J) \sum_{l \neq \alpha} \langle \langle n_{il\sigma} c_{i\alpha\sigma} | c_{j\beta\sigma}^\dagger \rangle \rangle, \end{aligned} \quad (4)$$

where the second-order Green's functions, such as $\langle \langle n_{il\bar{\sigma}} c_{i\alpha\sigma} | c_{j\beta\sigma}^\dagger \rangle \rangle$, appear on the right-hand side of Eq. (4). Further, we construct the equations of motion of all the second-order Green's functions that appear in Eq. (4), and the higher-order Green's

functions should emerge accordingly. To obtain a self-consistent loop for the calculation of the first-order Green's functions, some kinds of decoupling approximations should be introduced. Based on the Hubbard-I approximation [32] for the one-band Hubbard model, we develop a new decoupling scheme for the multi-orbital systems, such as

$$\begin{aligned}
\langle\langle n_{i\alpha\sigma'} c_{bm\sigma} | c_{j\beta\sigma}^\dagger \rangle\rangle &\approx \langle n_{i\alpha\sigma'} \rangle \langle\langle c_{bm\sigma} | c_{j\beta\sigma}^\dagger \rangle\rangle, \\
\langle\langle c_{bm\sigma}^\dagger c_{il\sigma} c_{i\alpha\sigma} | c_{j\beta\sigma}^\dagger \rangle\rangle &\approx \langle c_{bm\sigma}^\dagger c_{il\sigma} \rangle \langle\langle c_{i\alpha\sigma} | c_{j\beta\sigma}^\dagger \rangle\rangle \\
&\quad - \langle c_{bm\sigma}^\dagger c_{i\alpha\sigma} \rangle \langle\langle c_{il\sigma} | c_{j\beta\sigma}^\dagger \rangle\rangle, \\
\langle\langle n_{is\sigma'} n_{il\sigma''} c_{i\alpha\sigma} | c_{j\beta\sigma}^\dagger \rangle\rangle &\approx \langle n_{is\sigma'} \rangle \langle\langle n_{il\sigma''} c_{i\alpha\sigma} | c_{j\beta\sigma}^\dagger \rangle\rangle \\
&\quad + \langle n_{il\sigma''} \rangle \langle\langle n_{is\sigma'} c_{i\alpha\sigma} | c_{j\beta\sigma}^\dagger \rangle\rangle.
\end{aligned} \tag{5}$$

As a result, we can approximately express the higher-order Green's functions by the first-order Green's functions, making up a self-consistent loop for the calculation of the inhomogeneous Green's function \mathbf{G}

$$\mathbf{M} \cdot \mathbf{G} = \mathbf{N}, \tag{6}$$

where \mathbf{M} and \mathbf{N} are the same order matrices as \mathbf{G} , which can be obtained by

$$\langle AB \rangle = -\frac{1}{\pi} \int_{-\infty}^{+\infty} f(\omega) \text{Im} \langle\langle A | B \rangle\rangle. \tag{7}$$

By solving the above self-consistent equations, we obtain the real-space Green's function for a certain disordered configuration. From which we can also obtain the local density of states (LDOS) at site i for orbital α by $\rho_\alpha(\mathbf{r}_i, \omega) = -\frac{1}{\pi} \text{Im} G_{ii}^{\alpha\alpha}(\omega)$. To find the averaged DOS of the whole system, we need to calculate the LDOS of different disorder configurations, and then determine the sample-averaged values afterwards.

The DOS of Cu and Fe ions can be expressed respectively as

$$\begin{aligned}
\rho_\alpha^{(Fe)} &= \frac{1}{N_s} \sum_{s=1}^{N_s} \frac{1}{N_{Fe}} \sum_{i \in Fe} \rho_\alpha^{(s)}(\mathbf{r}_i, \omega) \\
\rho_\alpha^{(Cu)} &= \frac{1}{N_s} \sum_{s=1}^{N_s} \frac{1}{N_{Cu}} \sum_{i \in Cu} \rho_\alpha^{(s)}(\mathbf{r}_i, \omega),
\end{aligned} \tag{8}$$

where N_{Fe} and N_{Cu} represent the total numbers of the Fe and Cu ions, respectively. N_s is the number of disorder configurations. The real-space Green's function method has many advantages, such as simple in principle and suitable for many kinds of correlated compounds with disorder. In addition, we can perform self-consistent calculations for lattices with up to 32×32 sites.

3. Anderson Localization and Orbital Selectivity

Our method not only handles the lattice disorder precisely, but also treats the correlation more accurate than the mean-field approximation, making it a priority to deal with the correlated system with the presence of disorder. In this section, we use the newly developed real-space Green's function method to study the cooperative effect of multiorbital correlation and impurity-induced disorder on the OSMT.

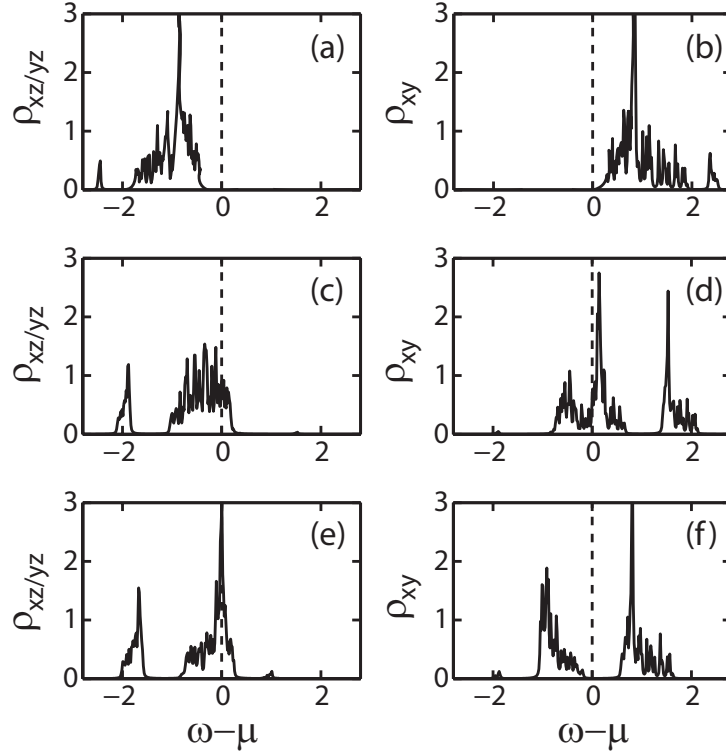


Figure 1. Density of states of d_{xz}/d_{yz} orbitals (left panel) and d_{xy} orbital (right panel) for the undoped cases with different Hund's rule couplings: $J=0.05$ eV (top panel), $J=0.18$ eV (middle panel), and $J=0.21$ eV (bottom panel). Top panel: a band insulator with fully filled d_{xz}/d_{yz} orbitals but empty d_{xy} orbital when $J=0.05$ eV; Middle panel: a metallic phase when $J=0.18$ eV, where all three orbitals are metallic; Bottom panel: an orbital-selective Mott phase when $J=0.21$ eV, where d_{xz}/d_{yz} orbitals are metallic, while d_{xy} orbital becomes a Mott insulator. The on-site correlation is $U=1.5$ eV, and the relation $U = U' + 2J$ is satisfied, as the same for the following figures.

3.1. OSMT tuned by Hund's rule coupling

A clear way to show the effect of Hund's rule coupling on the MIT is to omit the influence of the Cu substitution firstly. As the undoped Fe-based superconductors are indicated to have a filling of roughly two thirds based on the band structure calculations [6, 38], we determine the Fermi energy by a constraint of four electrons per Fe,

$$n_{total} = -\frac{1}{\pi} \sum_{i\alpha} \int_{-\infty}^{+\infty} f(\omega) \text{Im} G_{ii}^{\alpha\alpha}(\omega) d\omega = 4, \quad (9)$$

where $f(\omega)$ is the Fermi-Dirac distribution function. It was predicted that, only at half-filling, the Hund's rule coupling J is capable of strengthening the effective correlations to introduce a Mott-Hubbard MIT [7, 39, 40, 41]. In the undoped Fe-based superconductors, further research is needed to understand the effect of the Hund's rule coupling on the OSMT in a three-orbital system away from half-filling.

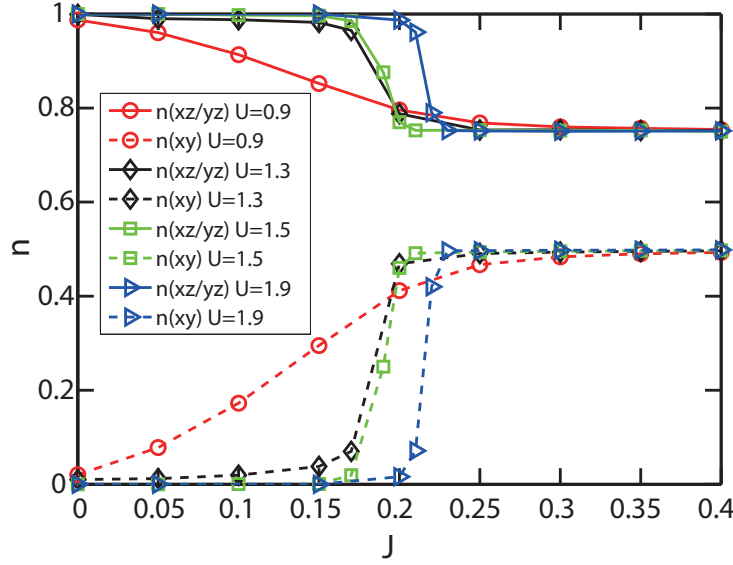


Figure 2. (Color online) Dependence of orbital occupancy on Hund's rule coupling J for undoped compounds with different interactions U . For very small J , it is a band insulator with fully-filled d_{xz}/d_{yz} orbitals but empty d_{xy} orbital. With the increase of the Hund's rule coupling, the difference of orbital occupancies becomes weak, and the d_{xy} orbital tends to be half-filled when J is larger than 0.2 eV, regardless of the value of U .

We study the influence of the Hund's rule coupling on the orbitally resolved DOS in undoped Fe-based superconductors, and the results are shown in Fig. 1. Consistent with the previous study [18], it is shown that the OSMT is manipulated by the Hund's rule coupling in the undoped Fe-based superconductors. As we can see in Fig. 1 (a) and (b), when the Hund's rule coupling is very small ($J=0.05$ eV), the system becomes a band insulator with the fully-filled d_{xz} and d_{yz} orbitals but the empty d_{xy} orbital, indicating that electrons prefer to occupy the orbitals of lower energy. With the increase of the Hund's rule coupling, all three orbitals become metallic shown in Fig. 1 (c) and (d) when $J=0.18$ eV, suggesting that electrons transfer from d_{xz} and d_{yz} orbitals to the empty d_{xy} orbital. Once J exceeds the critical value $J_c \approx 0.2$ eV, the Mott-Hubbard MIT happens in the d_{xy} orbital, while the d_{xz}/d_{yz} orbitals remain metallic, leading to an OSMT in the undoped Fe-based superconductor.

It is obvious that the electron transition from the d_{xz}/d_{yz} orbitals to d_{xy} orbital plays an essential role in finding the OSMP. We plot the effect of the Hund's rule coupling on the electron occupancy of each orbital in Fig. 2, where the crystal-field splitting is fixed as $\Delta_{xy}=0.75$ eV according to the local density calculations [33, 35]. As a result, the d_{xy} orbital locates much higher than the d_{xz}/d_{yz} orbitals, which leads to an extremely strong difference of orbital occupancies. However, the Hund's rule coupling favors orbital compensation, i.e., tends to equalize the different orbital populations. The OSMT appears as a result of the influence of the strong Hund's rule coupling J

overcoming the effect of the orbital level splitting Δ_{xy} [17, 42]. As shown in Fig. 2, the increase of Hund's rule coupling will decrease the difference of orbital occupancies generated by the orbital level splitting. The most remarkable portion is in the vicinity of $J=0.2$ eV, where the orbital occupancies change significantly, especially for the cases with large correlations U . When J is larger than 0.25 eV, the orbital occupancies tend to be stable and the d_{xy} orbital becomes half-filled.

In undoped Fe-based superconductors, the increase of Hund's rule coupling benefits the OSMT mainly in two aspects. First, the increase of Hund's rule coupling will transfer more electrons from the d_{xz}/d_{yz} orbitals to the d_{xy} orbital, causing the d_{xy} orbital half-filled and the d_{xz}/d_{yz} orbitals away from half-filled when $J > 0.2$ eV. Secondly, the Hund's rule coupling will enhance the effective correlations in the half-filled d_{xy} orbital when $J > 0.2$ eV. Therefore, the Mott-Hubbard MIT can happen only in the half-filled d_{xy} orbital, while the d_{xz}/d_{yz} orbitals are still metallic.

3.2. Cooperative effect of Hund's rule coupling and impurity-induced disorder

In this subsection, we study the effect of Cu substitution on the OSMT introduced by the Hund's rule coupling. In the Fe-based superconductors with the presence of Cu substitution, the electron occupations of Fe 3d orbitals will be manifestly affected by the impurities. In addition, it is found that impurity scattering introduced by Cu substitution has a strong effect on the electron transport, which can lead to Anderson MIT in iron-based compound. In Fig. 3, we present the effect of Cu substitution on the OSMT by comparing the orbitally resolved DOS for different doping concentrations ($x = 0.04$ and $x = 0.12$) with various Hund's couplings. Firstly, with the increase of Cu impurities, a slight broadening of the bandwidths is found for the band insulating phase with $J = 0.05$ eV. As a result, a small amount of electron states can be found across the Fermi level when $x = 0.12$ as shown by the insets in Fig. 3(a) and (b). On the contrary, we find that the Cu impurities can induce a pseudogap at the Fermi level for all three orbitals when $J = 0.18$ eV, as shown in Fig. 3(c) and (d).

The strong suppression on the DOS around Fermi level derives from the cooperative effect of multiorbital interactions and impurity-induced disorder. Efros and Shklovskii demonstrated that the interactions between the localized electrons in a disordered system can create a Coulomb gap in the DOS near the Fermi level [43]. Therefore, the appearance of the zero-bias anomaly at the Fermi energy is an evidence for the Anderson localization of electronic states in the correlated systems with disorder [44]. As some experiments show, as well as the density functional calculations demonstrate, some transition-metal substitutions can introduce localization effect in iron-based superconductors [45, 46, 47], which is consistent with our findings. Furthermore, the pseudogap in the d_{xz}/d_{yz} orbitals can still be found for the case with $J = 0.21$ eV (Fig. 3(e)) or $J = 0.25$ eV (Fig. 3(g)), which indicates that it is robust against the increasing Hund's rule coupling. In addition, the pseudogap will also affect the spectrum functions and Fermi surfaces significantly.

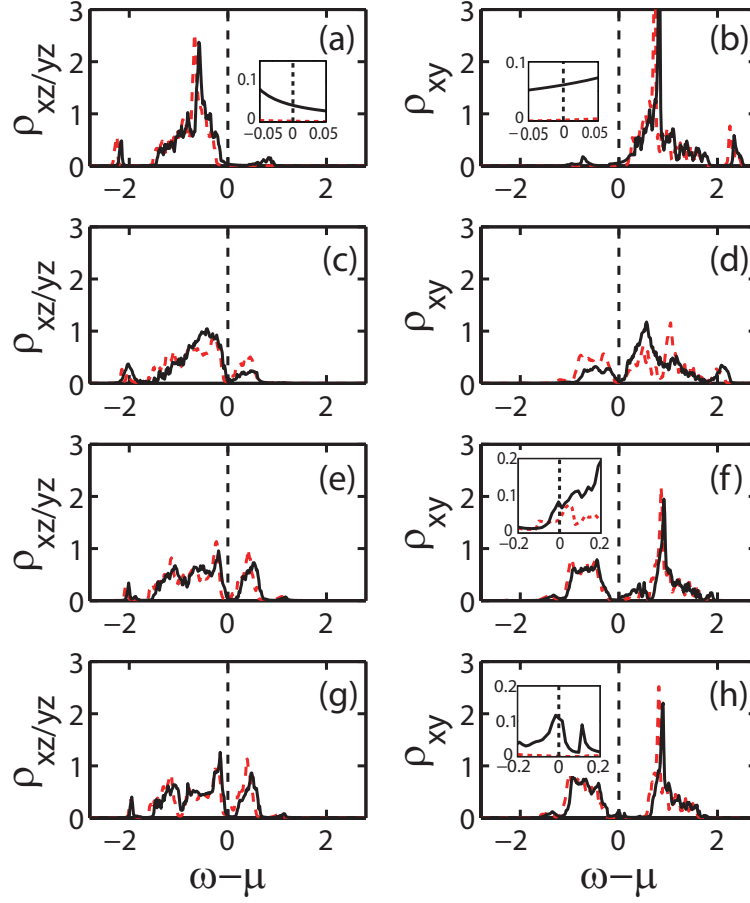


Figure 3. (Color online) Doping dependence of orbitally resolved density of states for different impurity concentrations: $x=0.04$ (dashed line) and $x=0.12$ (solid line). Top panel: a doping induced band insulator to Anderson insulator transition when $J=0.05$ eV; Second panel: Efros-shklovskii gap survives the strong impurity concentration when $J=0.18$ eV; Third panel: the influence of Cu substitution on the orbital selective Mott phase when $J=0.21$ eV, where the in-gap states are accumulated inside the Mott gap of the d_{xy} orbital; Bottom panel: an orbital-selective insulating phase appears in the lower doping case $x=0.04$ when $J=0.25$ eV, where the d_{xz}/d_{yz} orbitals are Anderson localized but the d_{xy} orbital is a Mott insulator. The system transfer to Anderson insulator with the the increase of doping concentration. Insets in (a), (b), (f), and (h): enlargement of the orbitally resolved density of states near the Fermi level. The correlations are $U=1.5$ eV and $u=3$ eV, and the results are averaged by 100 samples respectively.

In Fig. 4, we plot our result of the impurity effect on the spectrum functions for the cases with fixed Hund's rule coupling $J=0.18$ eV. Comparing with the undoped cases, we find an apparent broadening of the orbital bandwidths, especially for the d_{xy} orbital, in agreement with the experimental findings. This spectra-broadening behavior induced by the substitution has been experimentally observed in $\text{LiFe}_{1-x}\text{Co}_x\text{As}$ [48], $\text{NaFe}_{1-x}\text{Co}_x\text{As}$

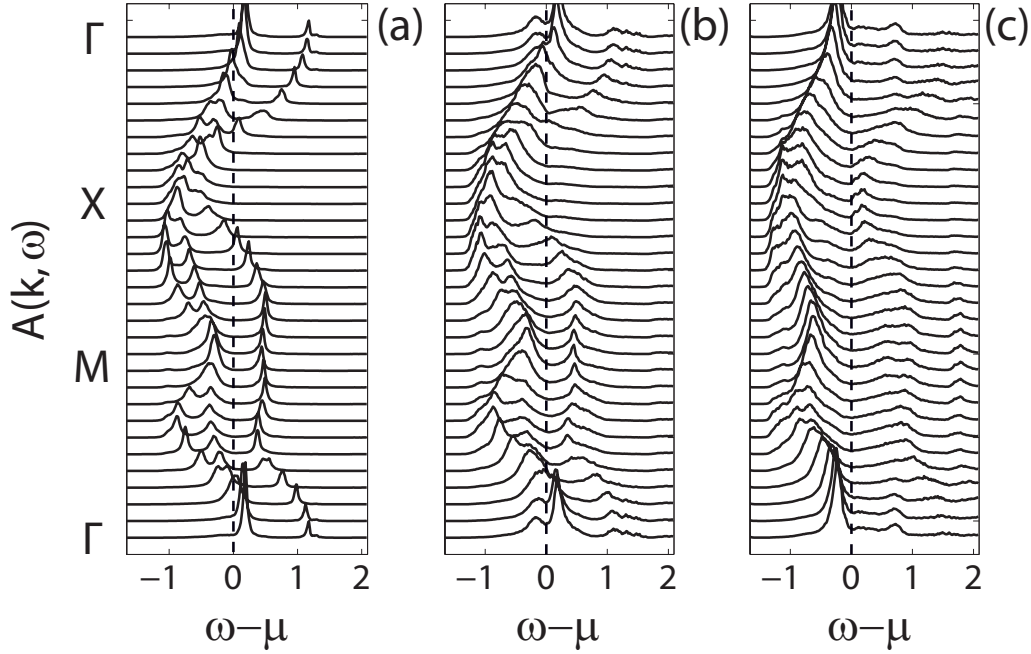


Figure 4. Spectrum functions for different substitution concentrations: $x=0.01$ (a), $x=0.04$ (b), and $x=0.08$ (c) when $J=0.18$ eV. The Fermi topology changes significantly with the increasing Cu concentration, and all Fermi pockets are pushed away from the Fermi level when $x=0.08$. The correlation parameters are $U=1.5$ eV and $u=3$ eV. Each result is obtained by averaging 100 disorder samples.

[49], and $\text{Fe}_{1.04}\text{Te}_{1-x}\text{Se}$ [50], which is believed to be an impurity-scattering effect induced by the dopants [51]. Once the dopants deviate from the Fe-plane, as the case of $\text{Ba}_{1-x}\text{K}_x\text{Fe}_2\text{As}_2$, the broadening effect disappears [52]. With the increase of doping concentration, we find that the top of band for the inner hole pocket shifts downward below the Fermi level, leading to the disappearance of the inner hole pocket, as shown in Fig. 4(b). It is worth noticing that this is just the embodiment of the appearance of the Efros-shklovskii gap at the Fermi surface. If the doping concentration is continuously increased, all bands will be pushed away from the Fermi level, leading all Fermi pockets vanish completely.

As for the OSMP introduced by the Hund's rule coupling in undoped Fe-based superconductors, the effect of Cu substitution will be mainly reflected in two aspects. One is to induce a pseudogap in the d_{xz}/d_{yz} orbitals, as shown in Fig. 3(e) and (g). The other effect is the appearance of the in-gap states in the d_{xy} orbital. Comparing Fig. 3(f) with Fig. 1(f), it is shown that, in the presence of Cu substitution, some electronic states will emerge inside the Mott gap of the d_{xy} orbital around the Fermi level. It is worth noting that these in-gap states are all localized, which can be confirmed directly from its origin. Through observing the real-space fluctuation of charge density induced by the substitution of copper ions, we find that the occupancy of the d_{xy} orbital

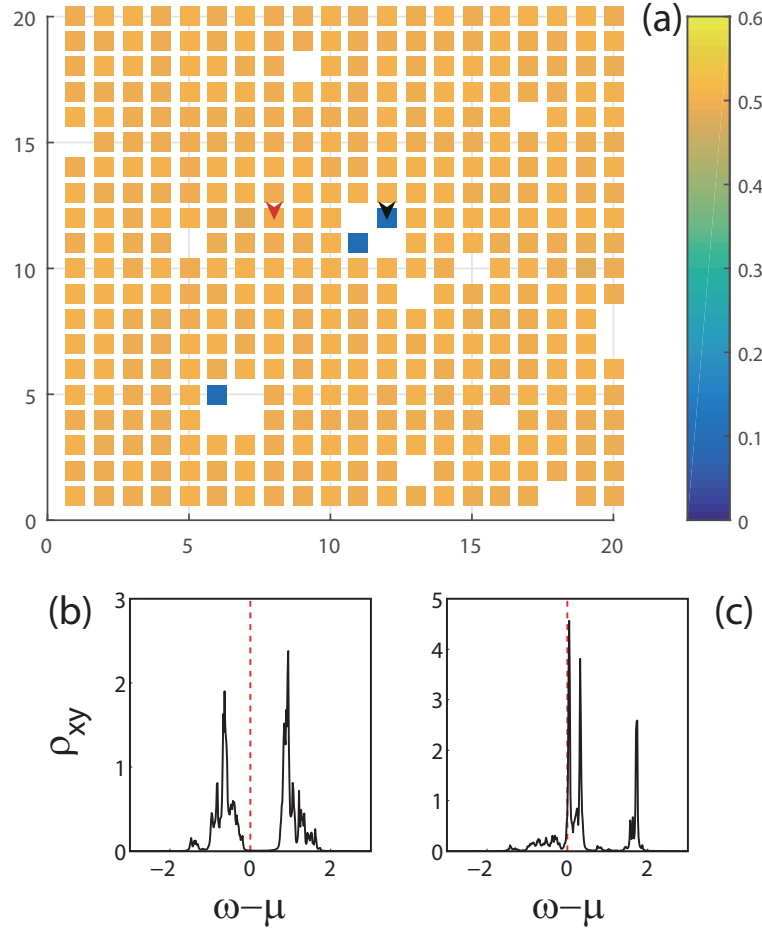


Figure 5. (Color online) The real-space distribution of the electron occupancy on d_{xy} orbital of iron atoms in a 20×20 lattice with 16 randomly selected Cu substitutions shown by the lattice vacancies. The value of n_{xy} decreases significantly to 0.1 at some specific sites which are very close to the highly concentrated area of the impurities. These specific sites aside the other sites remain to be half-filling. The LDOS of two representative sites, which are marked by red and black arrows, are shown in Fig (b) and (c) respectively. The correlation parameters are $U=1.5$ eV, $J=0.21$ eV, and $u=3$ eV.

deviates from half-filling at some discrete iron sites, which are indicated by blue (dark) squares in Fig. 5 (a). Obviously, these peculiar sites are easier to be found in the highly concentrated area of the impurities, where the real-space fluctuations induced by Cu substitution are much stronger. As a result, LDOS of these specific lattice points will be greatly changed. As shown in Fig. 5 (c) for the LDOS of a site with $n \approx 0.1$, it is found that the Mott gap is replaced by a sharp peak near the Fermi level, suggesting that the in-gap states in the DOS of the d_{xy} orbital are heavily localized. In contrast, the iron ions at most other sites will keep the d_{xy} orbital half-filled, where a Mott gap can be found at the Fermi level for the LDOS of the d_{xy} orbital, as shown in Fig. 5 (b) for the LDOS of a representative iron site.

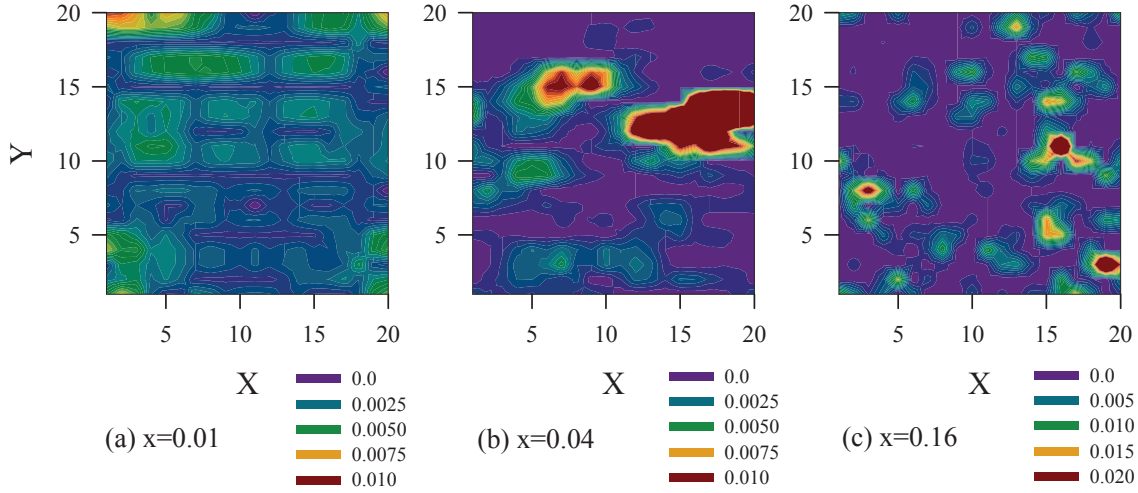


Figure 6. (Color online) For a certain disorder configuration of a 20×20 lattice, the real-space distribution of the LDOS is shown for an electronic state with energy very close to the Fermi level when the impurity concentration increases from $x = 0.01$ (a) to $x = 0.04$ (b), and to $x = 0.16$ (c). The localization of the electronic state is enhanced significantly with the increasing doping concentration. The correlation parameters are $U=1.5$ eV, $J=0.18$ eV, and $u=3$ eV.

To visually demonstrate the substitution-induced localization for all three orbitals, we show a real-space distribution of the LDOS of an electronic state with the energy very close to the Fermi level in Fig. 6 for a certain substitution configuration. In the case of a light doping ($x = 0.01$), it is shown that the LDOS distributes homogeneously in the real space, suggesting that the state is weakly localized. With the increase of the impurity concentration, the LDOS tends to be restricted in some small puddles, where the sizes of the puddles decrease significantly when the impurity concentration increases from $x = 0.04$ (Fig. 6(b)) to $x = 0.16$ (Fig. 6(c)). It is demonstrated that very strong Anderson localization has been introduced by the Cu substitutions in the cases of heavy doping.

In order to precisely determine the critical point of Anderson MIT, we perform the lattice-size scaling of the conductance g , which is obtained by a simplified form of Kubo formula in the case with $\omega = 0$ [53, 54],

$$g = \frac{e^2}{\pi} \text{Tr} [\text{Im}G_i(j, j') \text{Im}G_i(j' - 1, j - 1) + \text{Im}G_i(j - 1, j' - 1) \text{Im}G_i(j', j) - \text{Im}G_i(j, j' - 1) \text{Im}G_i(j', j - 1) - \text{Im}G_i(j - 1, j') \text{Im}G_i(j' - 1, j)], \quad (10)$$

where the trace is over the sites perpendicular to the current direction (k direction). (i, j) denote the coordinates of lattice sites in the ribbon, where the periodic boundary conditions should be applied only to the perpendicular direction to the current. j and j' are chosen to be on opposite sides of the lattice along the current direction, respectively. The conductance of the whole system is obtained by summarizing the three diagonal

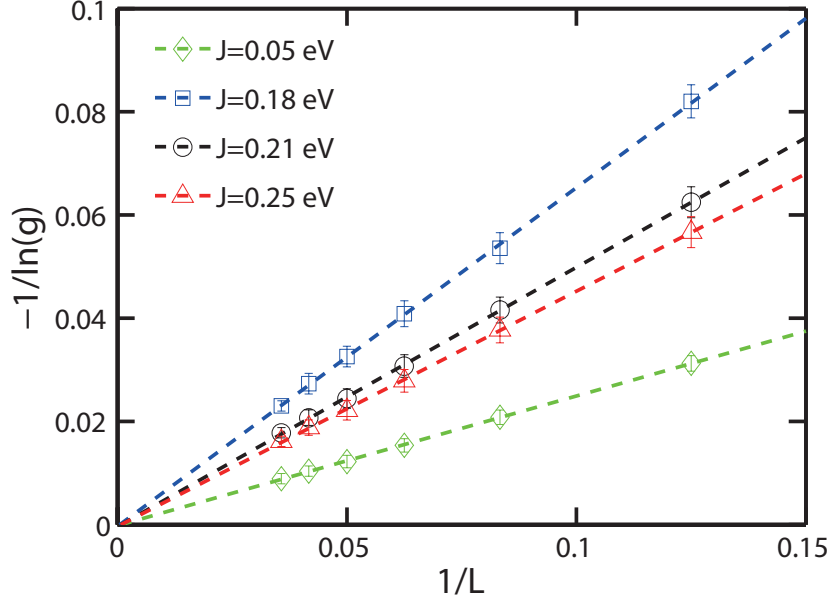


Figure 7. (Color online) Lattice-size scaling of conductance g : $-1/\ln(g)$ vs $1/L$ for different Hund's rule coupling. The linear fittings indicate that the conductance should decay exponentially with the lattice size. The doping concentration is $x=0.01$, and one hundred disordered samples are considered.

elements of the conductance matrix g , corresponding to the conductances of all three orbitals.

The conductance is expected to have the form $g \propto e^{-2L/\lambda}$ in an Anderson localized system [55], where λ is the localization length and L denotes the lattice size. In Fig. 7 we present the fitting of the lattice-size scaling of conductance of the weakly doped system ($x = 0.01$) for the cases with different Hund's rule coupling. We find linear relationship of $-1/\ln(g)$ vs $1/L$, suggesting that the system is Anderson localized for all cases with different Hund's rule coupling. In addition, no evidence of a significant delocalization effect of the Hund's rule coupling has been found, while a non-monotonic behavior is presented for the effect of J on the Anderson localization shown by the scaling of the conductance g . It is shown that the localization length decreases monotonously when the Hund's rule coupling increases from $J=0.18$ eV to $J=0.25$ eV. On the one hand, the Hund's rule coupling can lead to Mott-Hubbard MIT in the d_{xy} orbital. On the other hand, the Hund's rule coupling also has a strong effect to suppress the in-gap states around the Fermi level. As a result, the contribution of the d_{xy} orbital to the conductance will decrease with the increasing Hund's rule coupling. However, the situation is completely different when $J < 0.1$ eV. As shown in Fig. 1(a) and (b), the system behaves as a band insulator when $J < 0.1$ eV. Therefore, the conductance takes an extremely small value owing to the lack of states at the Fermi level. With the increase of the Hund's rule coupling, more and more electrons are transferred from the d_{xz}/d_{yz} orbitals to the d_{xy} orbital as shown in Fig. 2, accompanied with the increase of electronic states at the

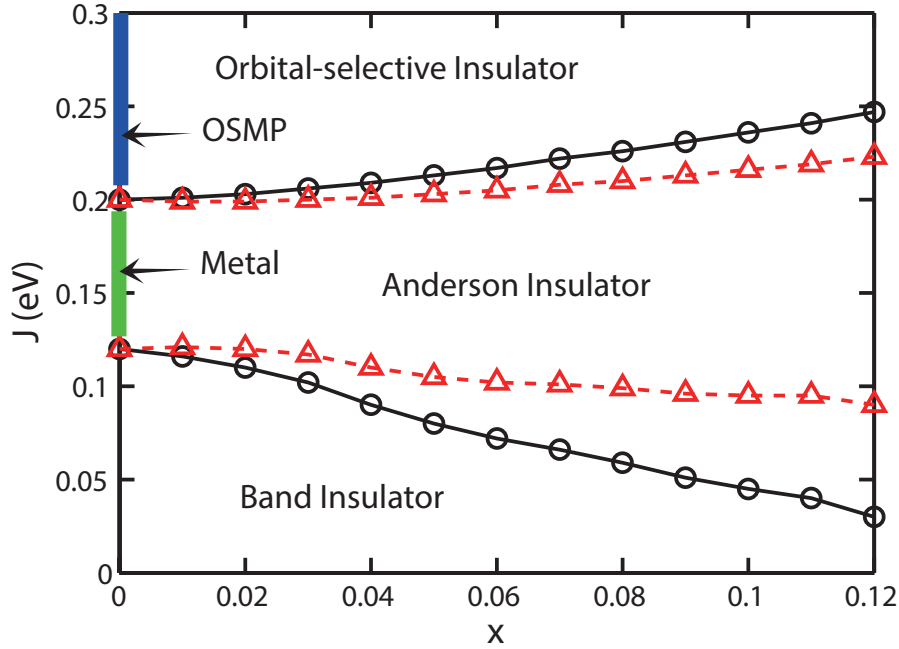


Figure 8. (Color online) Phase diagram of Cu-substituted iron-based superconductors. The solid lines with circles (dashed lines with triangles) indicate the phase boundaries of hole doping cases with $u=3$ eV (electron doping cases with $u=6$ eV).

Fermi level for all three orbitals. Therefore, the conductance increases firstly with the increasing Hund's rule coupling. While when the OSMT happens at about $J=0.21$ eV, a decrease of g can be found owing to enhancement of the suppression on the in-gap states with the increasing Hund's rule coupling.

We compile all our finding about the cooperative effect of the Hund's rule coupling and the doping-induced disorder on the MIT in a complete $J - x$ phase diagram, as shown in Fig. 8. An OSMP, where a Mott gap opens in the d_{xy} orbital but the degenerate d_{xz}/d_{yz} orbitals are still metallic, has been found in the undoped case when the Hund's coupling is $J=0.21$ eV. In the presence of Cu substitution, the Mott gap of the d_{xy} orbital is fulfilled by the in-gap states when x increases to 0.12, as shown in Fig. 3(f). However, If the Hund's rule coupling increases to $J=0.25$ eV, the doping induced in-gap states will be suppressed, even completely disappear in the case with $x=0.04$, as shown by the inset in Fig. 3(h). Therefore, we find an orbital-selective insulating phase under the impact of both disordered substitution and multi-orbital correlation, where the d_{xz}/d_{yz} orbitals are Anderson localized while the d_{xy} orbital is a Mott insulator. In addition, as indicated in Fig. 1(f) and Fig. 3(f), with the increase of the doping concentration, the whole multiorbital system will transfer from an orbital-selective insulator to an Anderson insulator when $J \geq 0.21$ eV. It is worth noticing that no metallic phase can be found for the Fe-based superconductor with the presence of Cu substitution. Based on the scaling theory [56], all states should be localized for arbitrary weak disorder in the two-dimensional systems. Our phase is consistent with this conclusion.

In our study, we find that when the on-site interactions u of Cu ions is larger than the critical value 5.2 eV, the hole doping will be converted into the electron doping [33]. However, the effects of Cu substitution on the OSMT are qualitatively the same for both the hole and electron dopants. Therefore, our study is mainly concentrated in the hole doping cases with $u=3$ eV. Besides, the carrier density will also be changed with the increasing Cu substitution. As a result, the area of the band insulator exhibits continued shrinkage with the increasing doping concentration, especially for the hole doping cases. The reason why the effect of the hole doping is more obvious than that of the electron doping is because the real-space fluctuation of the orbital occupancy is stronger in the hole doping cases. On the other hand, to suppress the in-gap states introduced by the Cu impurities, we should enhance the Hund's rule coupling to maintain the Mott gap. As a result, the boundary between the orbital-selective and Anderson insulating phases gradually moves upwards, owing to an increasing of the critical J_c for the Mott-Hubbard MIT transition in the d_{xy} orbital.

4. Conclusion

We study the cooperative effect of the Hund's rule coupling and the doping-induced disorder in iron-based superconductors with Cu substitution. The Hund's rule coupling benefits the orbital-selective Mott transition by transferring electrons from d_{xz}/d_{yz} orbitals to d_{xy} , and enhancing the correlation in the half-filled d_{xy} orbital as well. The Anderson localization introduced by the impurities is robust against variations in the Hund's rule coupling. A whole phase diagram depended on both the Hund's rule coupling and the doping concentration is obtained, where the Cu substitution affects the orbital-selective Mott phase by introducing localized in-gap states. As a result of the Anderson localization induced by the impurities, an orbital-selective insulating phase is found for the Cu-substituted Fe-based superconductors, where the d_{xy} orbital are Mott insulator while the degenerate d_{xz}/d_{yz} orbitals are Anderson localized.

Acknowledgments

We thank Prof. Liang-Jian Zou and Da-Yong Liu for helpful discussion. The computational resources utilized in this research were provided by Shanghai Supercomputer Center. The work was supported by National Natural Science Foundation of China (Nos. 10974018, 11174036 and 11474023), the National Basic Research Program of China (No. 2011CBA00108), and the Fundamental Research Funds for the Central Universities.

References

- [1] Lebegue S 2007 Phys. Rev.B 75 035110
- [2] Singh D J and Du M H 2008 Phys. Rev. Lett.100 237003

- [3] Kamihara Y, Hiramatsu H, Hirano M, Kawamura R, Yanagi H, Kamiya T and Hosono H 2006 J. Am. Chem. Soc. **128** 10012
- [4] Hirschfeld P J, Korshunov M M and Mazin I I 2011 Rep. Prog. Phys. **74** 124508
- [5] Chen X, Dai P, Feng D, Xiang T and Zhang F C 2014 Nat. Sci. Rev. **1** 371
- [6] Haule K, Kotliar G 2009 New J. Phys. **11** 025021
- [7] deMedici L 2011 Phys. Rev. B **83** 205112
- [8] deMedici L, Giovannetti G and Capone M 2014 Phys. Rev. Lett. **112** 177001
- [9] Fanfarillo L and Bascones E 2015 Phys. Rev. B **92** 075136
- [10] Yu R, Si Q 2013 Phys. Rev. Lett. **110** 146402
- [11] Yi M et al. 2015 Nat. Commun. 6:7777 doi: 10.1038/ncomms8777
- [12] Yi M, Lu D H, Yu R, Riggs S C, Chu J H, Lv B, Liu Z K, Lu M, Cui Y T, Hashimoto M, Mo S K, Hussain Z, Chu C W, Fisher I R, Si Q and Shen Z X 2013 Phys. Rev. Lett. **110** 067003
- [13] Wang Z, Schmidt M, Fischer J, Tsurkan V, Greger M, Vollhardt D, Loidl A and Deisenhofer J 2014 Nat. Commun. **5**:3202 doi:10.1038/ncomms4202
- [14] Ding X X, Pan Y M, Yang H, Wen H H 2014 Phys. Rev. B **89** 224515
- [15] Georges A, Kotliar G, Krauth W and Rozenberg M J 1996 Rev. Mod. Phys. **68** 13
- [16] Anisimov V I, Nekrasov I A, Kondakov D E, Rice T M and Sigrist M 2002 Eur. Phys. J. B **25** 191
- [17] Werner P, Millis A J 2007 Phys. Rev. Lett. **99** 126405
- [18] deMedici L, Hassan S R, Capone M and Dai X 2009 Phys. Rev. Lett. **102** 126401
- [19] Song Z Y, Lee H, and Zhang Y Z 2015 New J. Phys. **17** 033034
- [20] McLeod J A, Buling A, Green R J, Boyko T D, Skorikov N A, Kurmaev E Z, Neumann M, Finkelstein L D, Ni N, Thaler A, Bud'ko S L, Canfield P C and Moewes A 2012 J. Phys.: Condens. Matter **24** 215501
- [21] Yan Y J, Cheng P, Ying J J, Luo X G, Chen F, Zou H Y, Wang A F, Ye G J, Xiang Z J, Ma J Q and Chen X H 2013 Phys. Rev. B **87** 075105
- [22] Cheng P, Shen B, Han F and Wen H H 2013 Eur. Phys. Lett. **104** 37007
- [23] Ideta S, Yoshida T, Nishi I, Fujimori A, Kotani Y, Ono K, Nakashima Y, Yamaichi S, Sasagawa T, Nakajima M, Kihou K, Tomioka Y, Lee C H, Iyo A, Eisaki H, Ito T, Uchida S and Arita R 2013 Phys. Rev. Lett. **110** 107007
- [24] Merz M, Schweiss P, Nagel P, Wolf Th, Löhneysen H v and Schuppler S 2016 J. Phys. Soc. Jpn. **85** 044707
- [25] Wang A F, Lin J J, Cheng P, Ye G J, Chen F, Ma J Q, Lu X F, Lei B, Luo X G and Chen X H 2013 Phys. Rev. B **88** 094516
- [26] Cui S T, Kong S, Ju S L, Wu P, Wang A F, Luo X G, Chen X H, Zhang G B and Sun Z 2013 Phys. Rev. B **88** 245112
- [27] Huang T W, Chen T K, Yeh K W, Ke C T, Chen C L, Huang Y L, Hsu F C, Wu M K, Wu P M, Avdeev M and Studer A J 2010 Phys. Rev. B **82** 104502
- [28] Ni N, Thaler A, Yan J Q, Kracher A, Colombier E, Bud'ko S L and Canfield P C 2010 Phys. Rev. B **82** 024519
- [29] Li J, Guo Y F, Zhang S B, Yuan J, Tsujimoto Y, Wang X, Sathish C I, Sun Y, Yu S, Yi W, Yamaura K, Takayama-Muromachi E, Shirako Y, Akaogi M and Kontani H 2012 Phys. Rev. B **85** 214509
- [30] Williams A J, McQueen T M, Ksenofontov V, Felser C and Cava R J 2009 J. Phys.: Condens. Matter **21** 305701
- [31] Byczuk K, Hofstter W and Vollhard D 2010 Chapter 20 *50 years of Anderson Localization* ed. E. Abrahams (World Scientific)
- [32] Hubbard J 1963 Proc. Roy. Soc. A **276** 238
- [33] Liu Y, Liu D Y, Wang J L, Sun J, Song Y and Zou L J 2015 Phys. Rev. B **92** 155146
- [34] Daghofer M, Nicholson A, Moreo A and Dagotto E 2010 Phys. Rev. B **81** 014511
- [35] Daghofer M, Nicholson A and Moreo A 2012 Phys. Rev. B **85** 184515

- [36] Yi M, Lu D H, Moore R G, Kihou K, Lee C H, Iyo A, Eisaki H, Yoshida T, Fujimori A and Shen Z X 2012 *New J. Phys.* **14** 073019
- [37] Zubarev D N 1960 *Soviet Phys. Usp.* (English Transl.) **3** 320
- [38] Boeri L, Dolgov O V and Golubov A A 2008 *Phys. Rev. Lett.* **101** 026403
- [39] Han J E, Jarrell M and Cox D L 1998 *Phys. Rev. B* **58** R4199
- [40] Koga A, Imai Y and Kawakami N 2002 *Phys. Rev. B* **66** 165107
- [41] Pruschke T and Bulla R 2005 *Eur. Phys. J. B* **44** 217
- [42] Okamoto S, Millis A J 2004 *Phys. Rev. B* **70** 195120
- [43] Efros A L and Shklovskii B I 1975 *J. Phys. C: Solid State Phys.* **8** L49
- [44] Song Y, Bulut S, Wortis R and Atkinson W A 2009 *J. Phys.: Condens. Matter* **21** 385601
- [45] Wadati H, Elfimov I and Sawatzky G A 2010 *Phys. Rev. Lett.* **105** 157004
- [46] Yang H, Wang Z Y, Fang D L, Deng Q, Wang Q H, Xiang Y Y, Yang Y, Wen H H 2013 *Nat. Commun.* **4**:2749 doi: 10.1038/ncomms3749
- [47] Deng Q, Ding X X, Li S, Tao J, Yang H and Wen H H 2014 *New J. Phys.* **16** 063020
- [48] Pitcher M J, Lancaster T, Wright J D, Franke I, Steele A J, Baker P J, Pratt F L, Thomas W T, Parker D R, Blundell S J and Clarke S J 2010 *J. Am. Chem. Soc.* **132** 10467
- [49] Parker D R, Smith M J P, Lancaster T, Steele A J, Franke I, Baker P J, Pratt F L, Pitcher M J, Blundell S J and Clarke S J 2010 *Phys. Rev. Lett.* **104** 057007
- [50] Chen F, Zhou B, Zhang Y, Wei J, Ou H W, Zhao J F, He C, Ge Q Q, Arita M, Shimada K, Namatame H, Taniguchi M, Lu Z Y, Hu J, Cui X Y and Feng D L 2010 *Phys. Rev. B* **81** 014526
- [51] Ye Z R, Zhang Y, Chen F, Xu M, Jiang J, Niu X H, Wen C H P, Xing L Y, Wang X C, Jin C Q, Xie B P and Feng D L 2014 *Phys. Rev. X* **4** 031041
- [52] Chen H, Ren Y, Qiu Y, Bao W, Liu R H, Wu G, Wu T, Xie Y L, Wang X F, Huang Q and Chen X H 2009 *Europhys. Lett.* **85** 17006
- [53] Kubo B R 1957 *J. Phys. Soc. Jpn.* **12** 570
- [54] Lee P A and Fisher D S 1981 *Phys. Rev. Lett.* **47** 882
- [55] Kramer B and MacKinnon A 1993 *Rep. Prog. Phys.* **56** 1469
- [56] Lee P A and Ramakrishnan T V 1985 *Rev. Mod. Phys.* **57** 287